# Theoretical and experimental investigation of electron collisions with dimethyl sulfide

M. G. P. Homem,[1] I. Iga,[1] J. R. Ferraz,[2] A. S. dos Santos,[2] L. E. Machado,[2] G. L. C. de Souza,[3] L. M. Brescansin,[4] R. R. Lucchese,[5] and M.-T. Lee[1]

[1]*Departamento de Química, UFSCar, 13565-905 São Carlos, São Paulo, Brazil*
[2]*Departamento de Física, UFSCar, 13565-905 São Carlos, São Paulo, Brazil*
[3]*Departamento de Química, UFMT, 78060-900 Cuiabá, Mato Grosso, Brazil*
[4]*Instituto de Física "Gleb Wataghin," UNICAMP, 13083-970 Campinas, São Paulo, Brazil*
[5]*Chemistry Department, Texas A&M University, College Station, Texas 77842-3012, USA*

(Received 16 December 2014; published 30 January 2015)

We report a joint theoretical-experimental investigation of elastic electron scattering by dimethyl sulfide in the low- and intermediate-energy regions. More specifically, experimental differential, integral, and momentum-transfer cross sections are given in the 30–800 eV and $10^\circ - 130^\circ$ ranges. Theoretical cross sections are reported in the 1–500 eV interval. The experimental differential cross sections were determined using a crossed electron-beam–molecular-beam geometry, whereas the absolute values of the cross sections were obtained using the relative-flow technique. Theoretically, a complex optical potential was used to represent the collision dynamics, and a single-center expansion method combined with the Padé approximant method was used to solve the scattering equations. Our experimental data are in good agreement with the present calculated data but strongly disagree with those reported in a previous investigation.

DOI: 10.1103/PhysRevA.91.012713 PACS number(s): 34.80.Bm

## I. INTRODUCTION

From an environmental point of view, studies involving sulfur-containing compounds are relevant since many of them, such as hydrogen sulfide ($H_2S$), sulfur dioxide ($SO_2$), and sulfuric acid ($H_2SO_4$), are atmospheric pollutants and are responsible for the acidity of rain. In particular, one of the principal volatile sulfur-containing species, dimethyl sulfide (DMS) with the chemical formula $(CH_3)_2S$, is the major natural source of sulfur in the atmosphere [1]. It is produced in marine environments by biodegradation of organosulfur compounds and thus plays an important role in the atmospheric sulfur cycle. Probably for this reason, DMS has attracted considerable attention in both theoretical [2] and experimental investigations [3–9]. However, the only study up to now specifically concerning electron-DMS interaction is that reported by Rao *et al.* [8] in 2009. In that study, differential (DCS), integral (ICS), and momentum-transfer (MTCS) cross sections in the 30–500 eV energy range were reported for elastic electron scattering by DMS and also for dimethyl sulfoxide (DMSO). Rao *et al.* compared the experimental data only with their calculated results based on the independent-atom model (IAM) approach since there were no other experimental or theoretical cross-section determinations for these targets in the literature. It is interesting to note that double-dip structures are seen in their measured DCS for both DMS and DMSO at incident energies up to 100 eV. The authors attributed such structures to the occurrence of $d$-wave shape resonance during the collision processes. They justified such an occurrence based on the fact that the shape of the potential for electron interaction with both targets has a notable $3d$ character, and therefore a $d$-wave enhancement would increase the cross-section values through the medium angles as seen in their experiment [8]. The appearance of such double-dip structures in the measured DCS for DMS and DMSO at incident energies as high as 100 eV is, by itself, very interesting, although not confirmed by their IAM-based theory.

In order to understand the physical nature of the double-dip features, we performed a theoretical investigation of $e^-$-DMS scattering. In our calculation, the dynamics of the projectile-target interaction is represented by a molecular complex optical potential (MCOP) at the static-exchange-polarization plus absorption (SEPA) level of approximation. This model has already been applied by our group to study electron collisions with other sulfur-containing molecules, e.g., $H_2S$ [10] and $SO_2$ [11], and has successfully reproduced similar double-dip structures. For the sake of completeness, our calculations were carried out in the wide 1–500 eV energy range, thus providing cross-section data at energies below 30 eV, not covered in the Rao *et al.*'s article. Surprisingly, our DCS calculated in the 30–100 eV range do not present evidences of strong double-dip features. Quantitatively, there is also significant disagreement between our calculated results and their measured data, even at energies of hundreds of eV.

At energies above 75 eV, although their theoretical DCS calculated using the IAM agree fairly well with their experimental results, they strongly disagree with our calculation, even at 500 eV. This fact is quite surprising since it is expected that the results calculated using the IAM would converge to those calculated with more sophisticated methods at incident energies of hundreds of eV [12,13].

In order to solve such controversies, we decided to reinvestigate experimentally the elastic $e^-$-DMS scattering. Particularly, DCS are measured in the 30–800 eV energy range. These data are compared with the DCS of Rao *et al.* and with our theoretical results obtained using both the MCOP and the IAM-based method. Experimental ICS and MTCS are generated from the measured DCS via a numerical integration procedure.

The organization of this work is as follows: In Sec. II, we present briefly the experimental procedure. In Sec. III, the theory used and details of the calculations are presented. Finally, in Sec. IV, we present our calculated and measured data and compare them with the experimental and IAM data

 

of Rao *et al.* Some concluding remarks are also presented in that section.

## II. EXPERIMENT

The DMS used in the measurements was purchased from Sigma-Aldrich and had a purity higher than 99%. For each measurement, approximately 1 mL of the liquid sample was put into a small vial attached to the gas-handling manifold [14] and then underwent a pretreatment for elimination of atmospheric air through several freeze-thaw cycles. A gaseous DMS beam was formed by the saturated vapor above the liquid, and its purity was checked during the measurements using a residual gas analyzer attached to the electron spectrometer chamber.

The DCS was measured using the same experimental setup and procedure presented in several previous works [14–20]. Briefly, the intensities of the elastically scattered electrons were measured using a crossed electron-beam–molecular-beam geometry. The scattered electrons are energy filtered by a retarding-field energy analyzer with a resolution of about 1.5 eV. This analyzer discriminates the inelastically scattered electrons resulting from electronic excitation but not those from vibrational excitation. Therefore, our reported results are indeed vibrationally summed cross sections. Further, the scattered intensities are converted to absolute DCS using the relative-flow technique (RFT) [21] according to the procedure described in Refs. [14,17,20]. The application of RFT requires precise determination of the relative flows for both DMS and the secondary standards. They were measured according to the procedure described in Ref. [14]. In the present work, argon was used as a secondary standard. Specifically, the absolute DCS of Jansen *et al.* [22], with quoted experimental uncertainties of 6%, were used to normalize our data in the 100–500 eV range. In addition, at 50 and 800 eV, the absolute DCS of Dubois and Rudd [23] with uncertainties of 12% and the DCS reported by Williams and Willis [24] at 30 eV with quoted errors of 8% were used for normalization.

Our estimation of overall experimental uncertainties followed a procedure also given elsewhere [17–20]. Essentially, for the measured scattering intensities of each gas, the uncertainties of random nature (pressure fluctuations, electron-beam-current readings, background scattering, etc.) contributed less than 2% each; the statistical errors were estimated to be 3%. Additionally, there was still an uncertainty of 6% associated with the normalization procedure. The combination of all these contributions with the quoted uncertainties in the absolute DCS of the secondary standards [22–24] provided overall estimated uncertainties of 15% at 50 and 800 eV and 11% elsewhere.

In order to obtain ICS and MTCS, an extrapolation procedure was adopted to estimate DCS at scattering angles in the angular range not covered experimentally. In order to reduce the arbitrariness in this procedure we followed the trend of the theoretical results. The overall uncertainties on ICS and MTCS were estimated to be around 25% at 50 and 800 eV and 20% elsewhere.

## III. THEORY AND NUMERICAL PROCEDURE

The theory used in this work is essentially the same as that in several previous works [25–27]. Briefly, a complex optical potential $U_{\rm opt}$ composed of static ($U_{\rm st}$), exchange ($U_{\rm ex}$), correlation-polarization ($U_{\rm cp}$), and absorption ($U_{\rm ab}$) contributions was used to represent the electron-target interaction. Using this potential, the many-body nature of the electron-molecule interaction was reduced to a one-particle scattering problem. To solve this problem, $U_{\rm opt}$ was divided in two parts, namely, $U_1$ and $U_2$. Accordingly, the transition $T$ matrix can be written as

$$T = T_1 + T_2, \tag{1}$$

where

$$T_1 = \langle \phi(\vec{k}_f)|U_1|\psi_1^+(\vec{k}_i)\rangle \tag{2}$$

and

$$T_2 = \langle \psi_1^-(\vec{k}_f)|U_2|\psi^+(\vec{k}_i)\rangle. \tag{3}$$

In Eqs. (2) and (3), $\phi$ is the unperturbed plane wave, $\psi$ is the solution of the Schrödinger scattering equation for the full optical potential $U_{\rm opt}$, $\psi_1$ is the solution of the distorted-wave Schrödinger equation for potential $U_1$, and $k$ is the magnitude of the electron linear momentum. The partition of $U_{\rm opt}$ into $U_1$ and $U_2$ is arbitrary. In this work, we chose

$$U_1 = U_{\rm st} + U_{\rm ex}^{\rm loc} + U_{\rm cp} \tag{4}$$

and

$$U_2 = U_{\rm ex} - U_{\rm ex}^{\rm loc} + iU_{\rm ab}, \tag{5}$$

where $U_{\rm ex}^{\rm loc}$ is a reduced local exchange potential.

In the present work, $U_{\rm st}$ and $U_{\rm ex}$ were derived exactly from a near-Hartree-Fock self-consistent-field (HF-SCF) target wave function, whereas $U_{\rm cp}$ was obtained in the framework of the free-electron-gas model, derived from a parameter-free local density, as prescribed by Padial and Norcross [28]. The absorption potential $U_{\rm ab}$ is the scaled quasifree scattering model (SQFSM) absorption potential of Lee *et al.* [29], which is an improvement of version 3 of the model absorption potential originally proposed by Staszewska *et al.* [30]. The Hara free-electron-gas-exchange potential [31] was used to generate the local exchange potential $U_{\rm ex}^{\rm loc}$. Since $U_1$ is fully local, $\psi_1$ and $T_1$ were obtained by solving exactly the distorted-wave Schrödinger scattering equation via numerical procedures. Further, $T_2$ can be obtained iteratively using the $[N/N]$ Padé approximant technique [32],

$$T_2[N/N] = -\sum_{i,j=1,N-1} \langle \psi_1^-|U_2|\phi^{(i)+}\rangle (D^{-1})_{ij} \langle \phi^{(j)-}|U_2|\psi_1^+\rangle, \tag{6}$$

where

$$D_{ij} = \langle \phi^{(i)-}|U_2 - U_2 G_1^+ U_2|\phi^{(j)+}\rangle \tag{7}$$

and $G_1$ is the distorted wave Green's function, which satisfies the following condition:

$$(\nabla^2 + k^2 - U_1)G_1^{\pm}(\vec{r},\vec{r}') = \delta(\vec{r},\vec{r}'). \tag{8}$$

The superscripts $-$ and $+$ appearing in the above equations denote the incoming and outgoing boundary conditions of the scattering waves, respectively. In our calculation, the truncation parameter $N$ was iteratively increased until convergence was achieved. The converged body-frame (BF) $T$ matrix (or, equivalently, the BF scattering amplitude $f$) can then be

TABLE I. Experimental DCS (in $10^{-16}$ cm$^2$/sr) and ICS and MTCS (in $10^{-16}$ cm$^2$) for elastic $e^-$-DMS scattering.

| Angle | $E$ (eV) | | | | | | | | |
|---|---|---|---|---|---|---|---|---|---|
| (deg) | 30 | 50 | 100 | 150 | 200 | 300 | 400 | 500 | 800 |
| 10 | 32.04 | 28.37 | 18.78 | 11.10 | 9.43 | 9.12 | 7.01 | 5.09 | 4.48 |
| 15 | 14.01 | 10.49 | 6.28 | 3.91 | 3.53 | 2.92 | 2.37 | 2.17 | 1.88 |
| 20 | 6.73 | 4.56 | 1.99 | 1.81 | 1.83 | 1.35 | 1.35 | 1.21 | 0.909 |
| 25 | 4.02 | 2.64 | 1.26 | 1.23 | 1.10 | 0.84 | 0.855 | 0.591 | 0.545 |
| 30 | 2.59 | 1.79 | 0.922 | 0.690 | 0.618 | 0.526 | 0.413 | 0.349 | 0.322 |
| 40 | 1.789 | 1.08 | 0.493 | 0.373 | 0.266 | 0.214 | 0.251 | 0.161 | 0.101 |
| 45 | 1.61 | 0.883 | 0.359 | 0.289 | 0.192 | 0.191 | 0.181 | 0.105 | 0.076 |
| 50 | 1.44 | 0.612 | 0.289 | 0.187 | 0.149 | 0.129 | 0.131 | 0.086 | 0.053 |
| 60 | 1.02 | 0.379 | 0.187 | 0.133 | 0.104 | 0.083 | 0.080 | 0.055 | 0.034 |
| 70 | 0.713 | 0.332 | 0.132 | 0.106 | 0.084 | 0.057 | 0.049 | 0.037 | 0.025 |
| 80 | 0.810 | 0.330 | 0.121 | 0.076 | 0.057 | 0.037 | 0.034 | 0.028 | 0.019 |
| 90 | 0.800 | 0.266 | 0.115 | 0.063 | 0.038 | 0.026 | 0.026 | 0.021 | 0.017 |
| 100 | 0.742 | 0.260 | 0.091 | 0.053 | 0.028 | 0.026 | 0.024 | 0.017 | 0.015 |
| 110 | 0.546 | 0.231 | 0.079 | 0.040 | 0.028 | 0.026 | 0.027 | 0.017 | 0.013 |
| 120 | 0.519 | 0.249 | 0.089 | 0.043 | 0.037 | 0.031 | 0.027 | 0.018 | 0.012 |
| 130 | 0.554 | 0.308 | 0.128 | 0.058 | 0.046 | 0.041 | 0.029 | 0.019 | 0.011 |
| ICS | 20.5 | 14.6 | 11.2 | 8.2 | 7.4 | 6.4 | 5.2 | 4.4 | 2.8 |
| MTCS | 9.2 | 5.3 | 2.2 | 1.2 | 0.82 | 0.68 | 0.59 | 0.41 | 0.27 |

expressed in the laboratory frame (LF) by the usual frame transformation [33].

The HF-SCF wave function of DMS was obtained using the triple-zeta valence (TZV-3d) basis set of the GAMESS package [34]. At the experimental ground-state molecular geometry [35], this basis provided a total energy of −476.786114 hartrees. The calculated electric dipole moment was 1.7175 D, in fairly good agreement with the experimental value of 1.50 D [35]. Moreover, the asymptotic form of $U_{\rm cp}$ was generated with the dipole polarizabilities calculated at the HF-SCF level using the same basis set. The obtained values were $\alpha_{xx} = 53.06$ a.u., $\alpha_{yy} = 52.09$ a.u., and $\alpha_{zz} = 44.02$ a.u., resulting in an average dipole polarizability of $\alpha_0 = 49.72$ a.u., in good agreement with the experimental value of 50.95 a.u. [35]. In our calculation, the wave functions and interaction potentials, as well as the related matrices, were all single-center expanded about the center of mass of the molecule in terms of the well-known symmetry-adapted functions $X_{lh}^{p\mu}$ [36]. The truncation parameters used in these expansions were $l_c = 35$ and $h_c = 35$ for all bound and continuum orbitals, as well as for the $T$-matrix elements. The calculated cross sections were converged at $N$ up to 10. Since DMS is a polar system, the partial-wave expansions converged slowly due to the long-range nature of the dipole interaction potential. In order to overcome this difficulty, a Born-closure formula was used to account for the contribution of higher partial-wave components to the scattering amplitudes. The procedure used was the same as that in some of our previous studies [10,18,37].

In the IAM framework, the DCS for $e^-$-DMS scattering is written as

$$\frac{d\sigma}{d\Omega} = \sum_{i,j}^{N_a} f_i(\theta,k) f_j^*(\theta,k) \frac{\sin(sr_{ij})}{sr_{ij}}, \tag{9}$$

where $f_i(\theta,k)$ is the complex scattering amplitude due to the $i$th atom in a molecule, $r_{ij}$ is the internuclear distance between atoms $i$ and $j$, and $s = 2k\sin(\frac{\theta}{2})$ is the magnitude of the transferred momentum during the collision. The sum extends over the $N_a$ atoms of the molecule. The scattering amplitudes were obtained by solving the partial-wave radial Schödinger equation at the SEPA level of approximation:

$$\left(\frac{d^2}{dr^2} - \frac{l(l+1)}{r^2} - U_{\rm opt} + k^2\right) u_l(r) = 0. \tag{10}$$

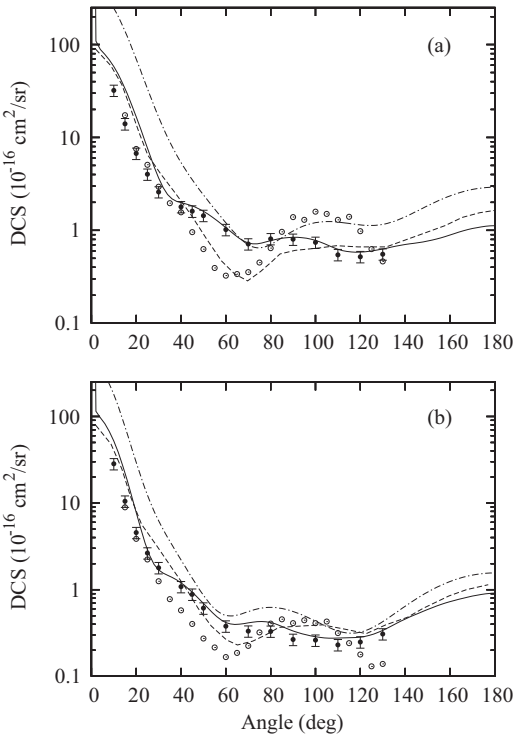


FIG. 1. DCS for elastic $e^-$-DMS scattering at (a) 30 eV and (b) 50 eV. Solid curve, present calculated data using the MCOP; dot-dashed curve, present calculated data using the IAM; dashed curve, IAM data of Rao *et al.* [8]; solid circles with error bars, present experimental data; open circles, measured data of Rao *et al.*

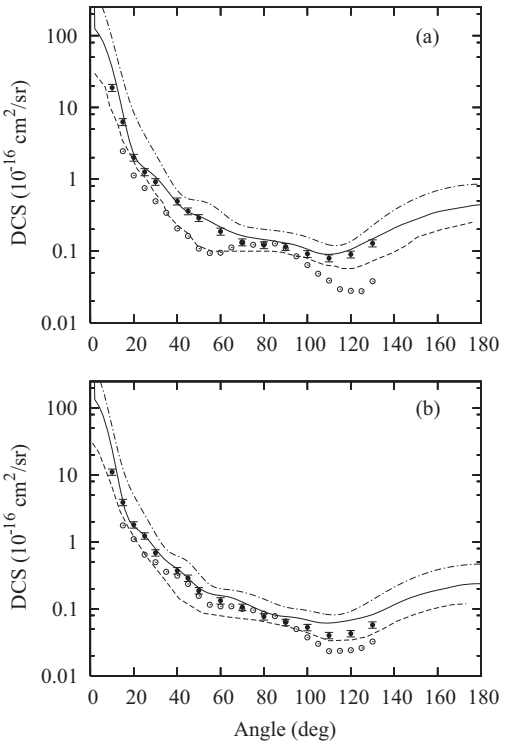


FIG. 2. Same as in Fig. 1, but at (a) 100 eV and (b) 150 eV.

The static atomic potentials were given by Salvat *et al.* [38], and a model potential proposed by Furness and McCarthy [39] was used to account for the exchange contributions.

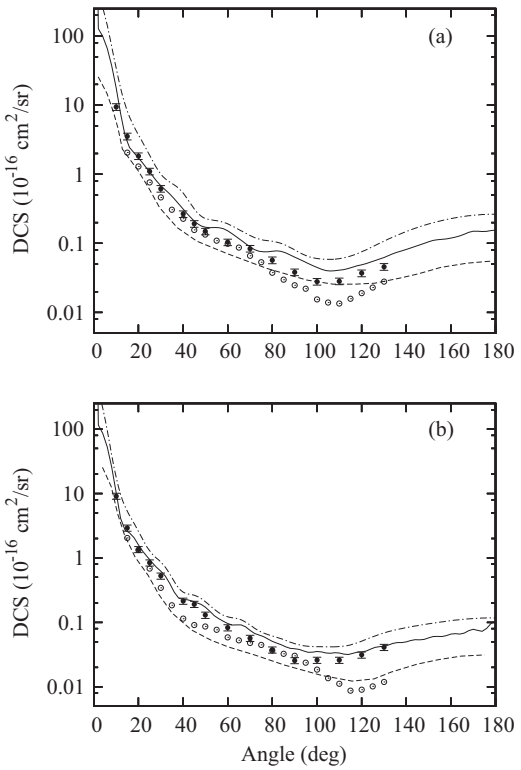


FIG. 3. Same as in Fig. 1, but at (a) 200 eV and (b) 300 eV.

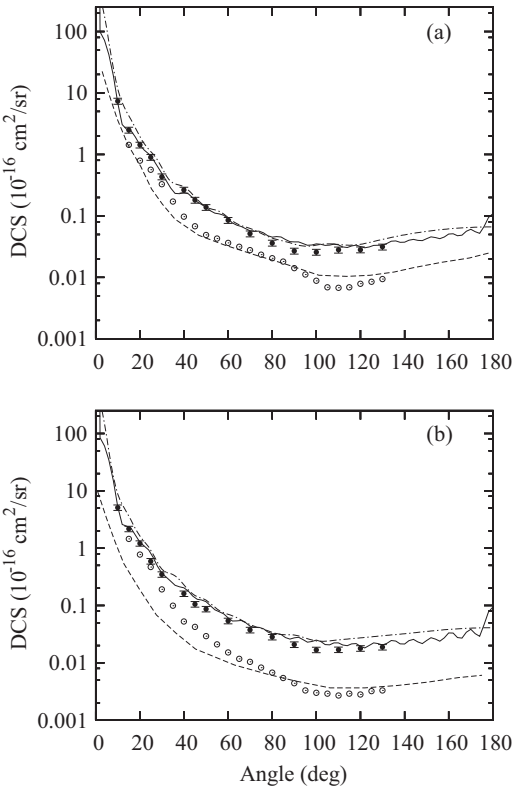


FIG. 4. Same as in Fig. 1, but at (a) 400 eV and (b) 500 eV.

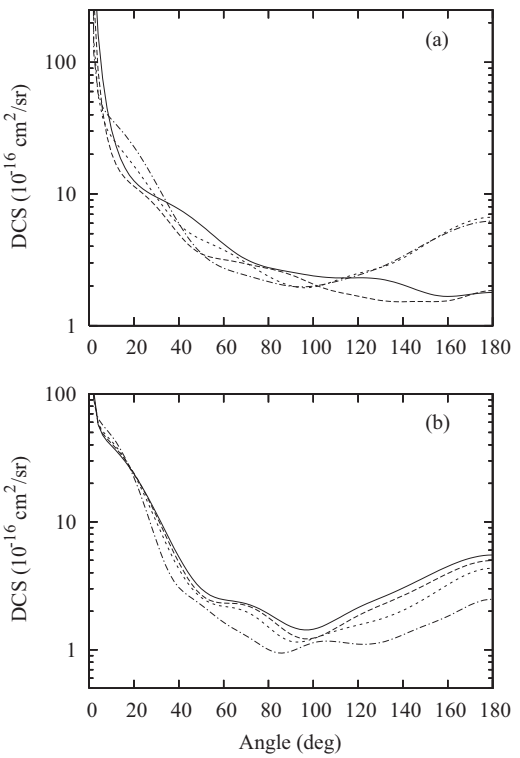


FIG. 5. Present theoretical MCOP DCS for elastic $e^-$-DMS scattering. (a) Solid curve, at 1 eV; long-dashed curve, at 2 eV; short-dashed curve, at 5 eV; dotted-dashed curve, at 8 eV. (b) Solid curve, at 10 eV; long-dashed curve, at 12 eV; short-dashed curve at 15 eV; dotted-dashed curve, at 20 eV.

The potential of Padial and Norcross [28] and the SQFSM absorption potential of Lee *et al.* [29] were used to account for the correlation-polarization and the absorption contributions, respectively. The atomic polarizabilities, as well as the internuclear distances used in the calculation, were taken from the literature [35,40].

## IV. RESULTS AND DISCUSSION

Our experimental DCS, ICS, and MTCS in the 30–800 eV range for elastic electron scattering by DMS are listed in Table I. In Figs. 1–4, we present a comparison of the present experimental and calculated MCOP DCS with the experimental data of Rao *et al.* [8] in the 30–500 eV energy range. The present calculated results using the IAM, as well as the IAM data of Rao *et al.*, are also shown. The comparison with the experimental data of Rao *et al.* is meaningful since their results are also vibrationally unresolved. It is seen that the present measured DCS disagree strongly with the experimental data of Rao *et al.*, both qualitatively and quantitatively, particularly at scattering angles larger than 40°. Moreover, no evidence of a pronounced double-dip structure is seen in our DCS in the 30–100 eV range. The best agreement between the two sets of experimental data occurs at 150 eV; however, their results are systematically lower than ours. Also at 300 eV and above, although the measured DCS of Rao *et al.* [8] agree qualitatively with our data, the magnitude of their DCS at large scattering angles lies well below. On the other hand, there is a very good qualitative agreement between our experimental data and the present calculated results using the MCOP. Quantitative agreement is also good, except at 30 and 50 eV, where our calculation overestimates the present experimental DCS at small scattering angles. At 400 and 500 eV, small oscillations are seen in our calculated data, particularly at large scattering angles. They are attributed to the lack of convergence in the partial-wave expansion of both the interaction potential and the $T$-matrix elements. Moreover, our calculated results using the IAM at 30 eV disagree qualitatively and quantitatively with both the present experimental data and calculated results using the MCOP. At higher energies, although there is a qualitative agreement between the results calculated using the IAM and MCOP, IAM-based calculations systematically overestimate the DCS. Nevertheless, the discrepancies between the two sets of theoretical data diminish with increasing incident energies, as expected [12,13]. Although there is an overall qualitative agreement between both IAM calculations, the magnitude of the IAM DCS reported by Rao *et al.* [8] is much smaller than the present IAM data, which is quite intriguing since the essence of the physics accounted for in both IAM calculations is quite similar. Actually, the lack of inclusion of absorption effects in their calculation would only increase the magnitude of DCS. Therefore we cannot explain the reason for such strong disagreement.

For the sake of completeness, in Fig. 5, we present some MCOP DCS in the 1–20 eV energy range. Unfortunately, there are neither experimental nor theoretical results to compare

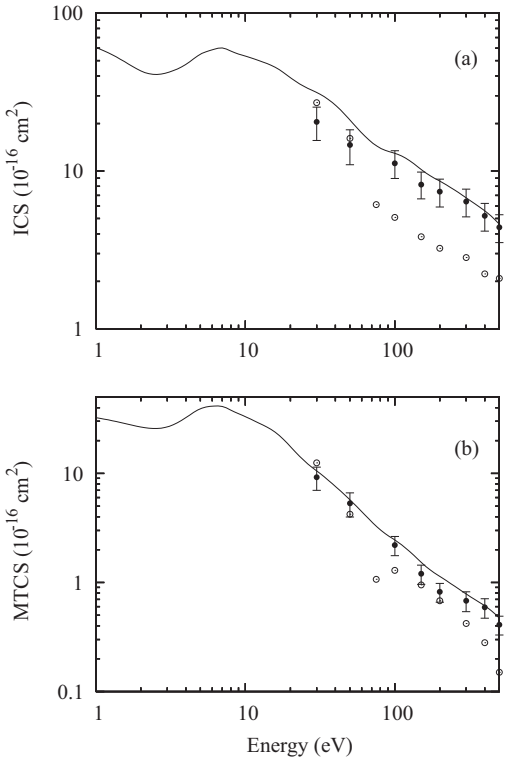


FIG. 6. (a) ICS and (b) MTCS for elastic $e^-$-DMS scattering in the 1–500 eV range. Solid curve, present calculated data using the MCOP; solid circles with error bars, present experimental data; open circles, measured data of Rao *et al.* [8].

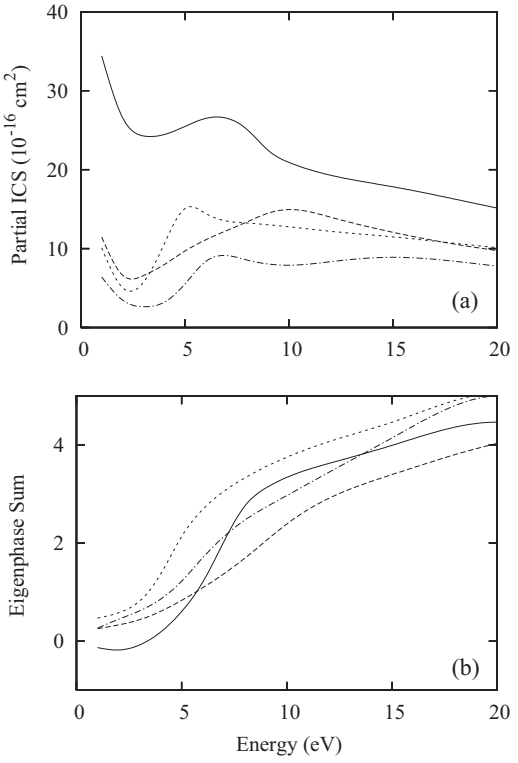


FIG. 7. Present partial-channel (a) ICS and (b) eigenphase sum calculated using the MCOP for elastic $e^-$-DMS scattering in the 1–20 eV energy range. Solid curve, for $A_1$ symmetry; dot-dashed curve, for $A_2$ symmetry; long-dashed curve, for $B_1$ symmetry; short-dashed curve, for $B_2$ symmetry.

with our data. It is interesting to note that in the energy interval between 10 and 15 eV, the calculated DCS do show some double-dip structure evidence, indicating the possible occurrence of $d$-wave resonance.

In Fig. 6, we present our theoretical ICS and MTCS calculated using the MCOP for electron scattering by DMS in the 1–500 eV energy range. The present experimental results of ICS and MTCS and those reported by Rao *et al.* [8] are also shown for comparison with our theoretical results. In general, there is good agreement between our calculated and measured data at 100 eV and above. Nevertheless, our calculation overestimates slightly the experimental ICS at 30 and 50 eV. On the other hand, the experimental ICS and MTCS reported by Rao *et al.* lie well below both our calculated and experimental results, except at 30 and 50 eV, where their results agree reasonably well with ours. However, considering the significant discrepancies between their measured DCS and ours at these energies, we conclude that this apparent good agreement is probably fortuitous.

At low incident energies, our calculated ICS and MTCS show a broad resonance-like feature centered at about 7 eV and a shoulder at about 15 eV. In order to clarify the physical nature of these features, we present in Figs. 7(a) and 7(b) the partial ICS (without Born correction) and the eigenphase sums. From Fig. 7, one may conclude that the feature located at about 7 eV, seen in Fig. 6, is a combination of $^2B_2$ (at 5 eV), $^2A_2$ (at 6.5 eV), and $^2A_1$ (at 7 eV) shape resonances, whereas that seen at about 15 eV is due to a broad $^2B_1$ (at 10 eV) shape resonance. Probably, the double-dip behavior seen in our calculated DCS in the 10–15 eV range can be associated with this $^2B_1$ resonance.

In summary, in this study, we report a joint theoretical-experimental investigation of electron collision with DMS in a wide energy range. More precisely, absolute DCS, ICS, and MTCS for elastic $e^-$-DMS scattering were reinvestigated experimentally in the 30–800 eV range. This investigation was mainly motivated by the strong disagreement between our theoretical cross sections calculated using the MCOP model and the existing experimental data [8]. As a result, it is seen that the present experimental DCS, ICS, and MTCS and those of Rao *et al.* show significant discrepancies. However, the reliability of the present measurement is supported by the MCOP calculations in the entire energy range covered herein and by the present IAM calculations at the higher end of the energies.

## ACKNOWLEDGMENTS

This research was partially supported by the agencies CNPq (Brazil), FAPESP (Brazil), and CAPES (Brazil).

[1] R. J. Charlson, J. E. Lovelock, M. O. Andreae, and S. G. Warren, Nature (London) **326**, 655 (1987).
[2] M. R. Manaa and D. R. Yarkony, J. Am. Chem. Soc. **116**, 11444 (1994).
[3] J. H. Lee, R. B. Timmons, and L. J. Stief, J. Chem. Phys. **64**, 300 (1976).
[4] P. Quintana, R. F. Delmdahl, D. H. Parker, B. Martínez-Haya, F. J. Aoiz, L. Bañares, and E. Verdasco, Chem. Phys. Lett. **325**, 146 (2000).
[5] Y. Zheng, J. Rolke, G. Cooper, and C. E. Brion, J. Electron Spectrosc. Relat. Phenom. **123**, 377 (2002).
[6] B. Martínez-Haya, P. Quintana, L. Bañares, P. Samartzis, D. J. Smith, and T. N. Kitsopoulos, J. Chem. Phys. **114**, 4450 (2001).
[7] P. Limão-Vieira, S. Eden, P. A. Kendall, N. J. Mason, and S. V. Hoffmann, Chem. Phys. Lett. **366**, 343 (2002).
[8] K. C. Rao, K. G. Bhushan, R. Mukund, S. C. Gadkari, and J. V. Yakhmi, Phys. Rev. A **79**, 062714 (2009).
[9] R. B. Bernini, L. B. G. da Silva, F. N. Rodrigues, L. H. Coutinho, A. B. Rocha, and G. G. B. de Souza, J. Chem. Phys. **136**, 144307 (2012).
[10] L. M. Brescansin, L. E. Machado, M.-T. Lee, H. Cho, and Y. S. Park, J. Phys. B **41**, 185201 (2008).
[11] L. E. Machado, R. T. Sugohara, A. S. dos Santos, M.-T. Lee, I. Iga, G. L. C. de Souza, M. G. P. Homem, S. E. Michelin, and L. M. Brescansin, Phys. Rev. A **84**, 032709 (2011).
[12] A. Jain, S. S. Tayal, L. C. G. Freitas, and M.-T. Lee, J. Phys. B **16**, L99 (1983).
[13] M.-T. Lee, L. M. Brescansin, M. A. P. Lima, L. E. Machado, and E. P. Leal, J. Phys. B **23**, 4331 (1990).
[14] M. G. P. Homem, I. Iga, R. T. Sugohara, I. P. Sanches, and M. T. Lee, Rev. Sci. Instrum. **82**, 013109 (2011).
[15] I. Iga, M. T. Lee, M. G. P. Homem, L. E. Machado, and L. M. Brescansin, Phys. Rev. A **61**, 022708 (2000).
[16] P. Rawat, I. Iga, M. T. Lee, L. M. Brescansin, M. G. P. Homem, and L. E. Machado, Phys. Rev. A **68**, 052711 (2003).
[17] R. T. Sugohara, M. G. P. Homem, I. P. Sanches, A. F. de Moura, M. T. Lee, and I. Iga, Phys. Rev. A **83**, 032708 (2011).
[18] M.-T. Lee, G. L. C. de Souza, L. E. Machado, L. M. Brescansin, A. S. dos Santos, R. R. Lucchese, R. T. Sugohara, M. G. P. Homem, I. P. Sanches, and I. Iga, J. Chem. Phys. **136**, 114311 (2012).
[19] R. T. Sugohara, M. G. P. Homem, I. Iga, G. L. C. de Souza, L. E. Machado, J. R. Ferraz, A. S. dos Santos, L. M. Brescansin, R. R. Lucchese, and M.-T. Lee, Phys. Rev. A **88**, 022709 (2013).
[20] M. G. P. Homem, R. T. Sugohara, I. P. Sanches, M. T. Lee, and I. Iga, Phys. Rev. A **80**, 032705 (2009).
[21] S. K. Srivastava, A. Chutjian, and S. Trajmar, J. Chem. Phys. **63**, 2659 (1975).
[22] R. H. J. Jansen, F. J. de Heer, H. J. Luyken, B. van Wingerden, and H. J. Blaauw, J. Phys. B **9**, 185 (1976).
[23] R. D. DuBois and M. E. Rudd, J. Phys. B **9**, 2657 (1976).
[24] J. F. Williams and B. A. Willis, J. Phys. B **9**, 1670 (1975).
[25] P. Rawat, M. G. P. Homem, R. T. Sugohara, I. P. Sanches, I. Iga, G. L. C. de Souza, A. S. dos Santos, R. R. Lucchese, L. E. Machado, L. M. Brescansin, and M.-T. Lee, J. Phys. B **43**, 225202 (2010).
[26] G. L. C. de Souza, M.-T. Lee, I. P. Sanches, P. Rawat, I. Iga, A. S. dos Santos, L. E. Machado, R. T. Sugohara, L. M. Brescansin, M. G. P. Homem, and R. R. Lucchese, Phys. Rev. A **82**, 012709 (2010).
[27] J. R. Ferraz, A. S. dos Santos, G. L. C. de Souza, A. I. Zanelato, T. R. M. Alves, M.-T. Lee, L. M. Brescansin, R. R. Lucchese, and L. E. Machado, Phys. Rev. A **87**, 032717 (2013).

[28] N. T. Padial and D. W. Norcross, Phys. Rev. A **29**, 1742 (1984).
[29] M.-T. Lee, I. Iga, L. E. Machado, L. M. Brescansin, E. A. y Castro, I. P. Sanches, and G. L. C. de Souza, J. Electron Spectrosc. Relat. Phenom. **155**, 14 (2007).
[30] G. Staszewska, D. W. Schwenke, and D. G. Truhlar, Phys. Rev. A **29**, 3078 (1984).
[31] S. Hara, J. Phys. Soc. Jpn. **22**, 710 (1967).
[32] F. A. Gianturco, R. R. Lucchese, and N. Sanna, J. Chem. Phys. **102**, 5743 (1995).
[33] A. R. Edmonds, *Angular Momentum and Quantum Mechanics* (Princeton University Press, Princeton, NJ, 1960).
[34] M. W. Schmidt, K. K. Baldridge, J. A. Boatz, S. T. Elbert, M. S. Gordon, J. H. Jensen, S. Koseki, N. Matsunaga, K. A. Nguyen, S. Su, T. L. Windus, M. Dupuis, and J. A. Montgomery, J. Comput. Chem. **14**, 1347 (1993).
[35] NIST Computational Chemistry Comparison and Benchmark Database, http://cccbdb.nist.gov.
[36] P. G. Burke, N. Chandra, and F. A. Gianturco, J. Phys. B **5**, 2212 (1972).
[37] L. E. Machado, L. M. Brescansin, I. Iga, and M.-T. Lee, Eur. Phys. J. D **33**, 193 (2005).
[38] F. Salvat, J. D. Martínez, R. Mayol, and J. Parellada, Phys. Rev. A **36**, 467 (1987).
[39] J. B. Furness and I. E. McCarthy, J. Phys. B **6**, 2280 (1973).
[40] *Handbook of Chemistry and Physics*, 73rd ed., edited by D. R. Lide (CRC Press, Boca Raton, FL, 1992).